

Model independent determination of the spin of the Ω^- and its polarization alignment in $\psi(3686) \rightarrow \Omega^- \bar{\Omega}^+$

- M. Ablikim¹, M. N. Achasov^{10,c}, P. Adlarson⁶⁴, S. Ahmed¹⁵, M. Albrecht⁴, A. Amoroso^{63A,63C}, Q. An^{60,48}, Anita²¹, Y. Bai⁴⁷, O. Bakina²⁹, R. Baldini Ferroli^{23A}, I. Balossino^{24A}, Y. Ban^{38,k}, K. Begzsuren²⁶, J. V. Bennett⁵, N. Berger²⁸, M. Bertani^{23A}, D. Bettone^{24A}, F. Bianchi^{63A,63C}, J. Biernat⁶⁴, J. Bloms⁵⁷, A. Bortone^{63A,63C}, I. Boyko²⁹, R. A. Briere⁵, H. Cai⁶⁵, X. Cai^{1,48}, A. Calcaterra^{23A}, G. F. Cao^{1,52}, N. Cao^{1,52}, S. A. Cetin^{51B}, J. F. Chang^{1,48}, W. L. Chang^{1,52}, G. Chelkov^{29,b}, D. Y. Chen⁶, G. Chen¹, H. S. Chen^{1,52}, M. L. Chen^{1,48}, S. J. Chen³⁶, X. R. Chen²⁵, Y. B. Chen^{1,48}, W. S. Cheng^{63C}, G. Cibinetto^{24A}, F. Cossio^{63C}, X. F. Cui³⁷, H. L. Dai^{1,48}, J. P. Dai^{42,g}, X. C. Dai^{1,52}, A. Dbeysi¹⁵, R. B. de Boer⁴, D. Dedovich²⁹, Z. Y. Deng¹, A. Denig²⁸, I. Denysenko²⁹, M. Destefanis^{63A,63C}, F. De Mori^{63A,63C}, Y. Ding³⁴, C. Dong³⁷, J. Dong^{1,48}, L. Y. Dong^{1,52}, M. Y. Dong^{1,48,52}, S. X. Du⁶⁸, J. Fang^{1,48}, S. S. Fang^{1,52}, Y. Fang¹, R. Farinelli^{24A}, L. Fava^{63B,63C}, F. Feldbauer⁴, G. Felici^{23A}, C. Q. Feng^{60,48}, M. Fritsch⁴, C. D. Fu¹, Y. Fu¹, X. L. Gao^{60,48}, Y. Gao⁶¹, Y. Gao^{38,k}, Y. G. Gao⁶, I. Garzia^{24A,24B}, E. M. Gersabeck⁵⁵, A. Gilman⁵⁶, K. Goetzen¹¹, L. Gong³⁷, W. X. Gong^{1,48}, W. Gradl²⁸, M. Greco^{63A,63C}, L. M. Gu³⁶, M. H. Gu^{1,48}, S. Gu², Y. T. Gu¹³, C. Y. Guan^{1,52}, A. Q. Guo²², L. B. Guo³⁵, R. P. Guo⁴⁰, Y. P. Guo²⁸, Y. P. Guo^{9,h}, A. Guskov²⁹, S. Han⁶⁵, T. T. Han⁴¹, T. Z. Han^{9,h}, X. Q. Hao¹⁶, F. A. Harris⁵³, K. L. He^{1,52}, F. H. Heinsius⁴, T. Held⁴, Y. K. Heng^{1,48,52}, M. Himmelreich^{11,f}, T. Holtmann⁴, Y. R. Hou⁵², Z. L. Hou¹, H. M. Hu^{1,52}, J. F. Hu^{42,g}, T. Hu^{1,48,52}, Y. Hu¹, G. S. Huang^{60,48}, L. Q. Huang⁶¹, X. T. Huang⁴¹, Z. Huang^{38,k}, N. Huesken⁵⁷, T. Hussain⁶², W. Ikegami Andersson⁶⁴, W. Imoehl²², M. Irshad^{60,48}, S. Jaeger⁴, S. Janchiv^{26,j}, Q. Ji¹, Q. P. Ji¹⁶, X. B. Ji^{1,52}, X. L. Ji^{1,48}, H. B. Jiang⁴¹, X. S. Jiang^{1,48,52}, X. Y. Jiang³⁷, J. B. Jiao⁴¹, Z. Jiao¹⁸, S. Jin³⁶, Y. Jin⁵⁴, T. Johansson⁶⁴, N. Kalantar-Nayestanaki³¹, X. S. Kang³⁴, R. Kappert³¹, M. Kavatsyuk³¹, B. C. Ke^{43,1}, I. K. Keshk⁴, A. Khoukaz⁵⁷, P. Kiese²⁸, R. Kiuchi¹, R. Kliemt¹¹, L. Koch³⁰, O. B. Kolcu^{51B,e}, B. Kopf⁴, M. Kuemmel⁴, M. Kuessner⁴, A. Kupsc⁶⁴, M. G. Kurth^{1,52}, W. Kühn³⁰, J. J. Lane⁵⁵, J. S. Lange³⁰, P. Larin¹⁵, L. Lavezzi^{63C}, H. Leithoff²⁸, M. Lellmann²⁸, T. Lenz²⁸, C. Li³⁹, C. H. Li³³, Cheng Li^{60,48}, D. M. Li⁶⁸, F. Li^{1,48}, G. Li¹, H. B. Li^{1,52}, H. J. Li^{9,h}, J. L. Li⁴¹, J. Q. Li⁴, Ke Li¹, L. K. Li¹, Lei Li³, P. L. Li^{60,48}, P. R. Li³², S. Y. Li⁵⁰, W. D. Li^{1,52}, W. G. Li¹, X. H. Li^{60,48}, X. L. Li⁴¹, Z. B. Li⁴⁹, Z. Y. Li⁴⁹, H. Liang^{60,48}, H. Liang^{1,52}, Y. F. Liang⁴⁵, Y. T. Liang²⁵, L. Z. Liao^{1,52}, J. Libby²¹, C. X. Lin⁴⁹, B. Liu^{42,g}, B. J. Liu¹, C. X. Liu¹, D. Liu^{60,48}, D. Y. Liu^{42,g}, F. H. Liu⁴⁴, Fang Liu¹, Feng Liu⁶, H. B. Liu¹³, H. M. Liu^{1,52}, Huanhuan Liu¹, Huihui Liu¹⁷, J. B. Liu^{60,48}, J. Y. Liu^{1,52}, K. Liu¹, K. Y. Liu³⁴, Ke Liu⁶, L. Liu^{60,48}, Q. Liu⁵², S. B. Liu^{60,48}, Shuai Liu⁴⁶, T. Liu^{1,52}, X. Liu³², Y. B. Liu³⁷, Z. A. Liu^{1,48,52}, Z. Q. Liu⁴¹, Y. F. Long^{38,k}, X. C. Lou^{1,48,52}, F. X. Lu¹⁶, H. J. Lu¹⁸, J. D. Lu^{1,52}, J. G. Lu^{1,48}, X. L. Lu¹, Y. Lu¹, Y. P. Lu^{1,48}, C. L. Luo³⁵, M. X. Luo⁶⁷, P. W. Luo⁴⁹, T. Luo^{9,h}, X. L. Luo^{1,48}, S. Lusso^{63C}, X. R. Lyu⁵², F. C. Ma³⁴, H. L. Ma¹, L. L. Ma⁴¹, M. M. Ma^{1,52}, Q. M. Ma¹, R. Q. Ma^{1,52}, R. T. Ma⁵², X. N. Ma³⁷, X. X. Ma^{1,52}, X. Y. Ma^{1,48}, Y. M. Ma⁴¹, F. E. Maas¹⁵, M. Maggiore^{63A,63C}, S. Maldaner²⁸, S. Malde⁵⁸, Q. A. Malik⁶², A. Mangoni^{23B}, Y. J. Mao^{38,k}, Z. P. Mao¹, S. Marcello^{63A,63C}, Z. X. Meng⁵⁴, J. G. Messchendorp³¹, G. Mezzadri^{24A}, T. J. Min³⁶, R. E. Mitchell²², X. H. Mo^{1,48,52}, Y. J. Mo⁶, N. Yu. Muchnoi^{10,c}, H. Muramatsu⁵⁶, S. Nakhoul^{11,f}, Y. Nefedov²⁹, F. Nerling^{11,f}, I. B. Nikolaev^{10,c}, Z. Ning^{1,48}, S. Nisar^{8,i}, S. L. Olsen⁵², Q. Ouyang^{1,48,52}, S. Pacetti^{23B}, X. Pan⁴⁶, Y. Pan⁵⁵, A. Pathak¹, P. Patteri^{23A}, M. Pelizaeus⁴, H. P. Peng^{60,48}, K. Peters^{11,f}, J. Pettersson⁶⁴, J. L. Ping³⁵, R. G. Ping^{1,52}, A. Pitka⁴, R. Poling⁵⁶, V. Prasad^{60,48}, H. Qi^{60,48}, H. R. Qi⁵⁰, M. Qi³⁶, T. Y. Qi², S. Qian^{1,48}, W.-B. Qian⁵², Z. Qian⁴⁹, C. F. Qiao⁵², L. Q. Qin¹², X. P. Qin¹³, X. S. Qin⁴, Z. H. Qin^{1,48}, J. F. Qiu¹, S. Q. Qu³⁷, K. H. Rashid⁶², K. Ravindran²¹, C. F. Redmer²⁸, A. Rivetti^{63C}, V. Rodin³¹, M. Rolo^{63C}, G. Rong^{1,52}, Ch. Rosner¹⁵, M. Rump⁵⁷, A. Sarantsev^{29,d}, Y. Schelhaas²⁸, C. Schnier⁴, K. Schoenning⁶⁴, D. C. Shan⁴⁶, W. Shan¹⁹, X. Y. Shan^{60,48}, M. Shao^{60,48}, C. P. Shen², P. X. Shen³⁷, X. Y. Shen^{1,52}, H. C. Shi^{60,48}, R. S. Shi^{1,52}, X. Shi^{1,48}, X. D. Shi^{60,48}, J. J. Song⁴¹, Q. Q. Song^{60,48}, W. M. Song²⁷, Y. X. Song^{38,k}, S. Sosio^{63A,63C}, S. Spataro^{63A,63C}, F. F. Sui⁴¹, G. X. Sun¹, J. F. Sun¹⁶, L. Sun⁶⁵, S. S. Sun^{1,52}, T. Sun^{1,52}, W. Y. Sun³⁵, Y. J. Sun^{60,48}, Y. K. Sun^{60,48}, Y. Z. Sun¹, Z. T. Sun¹, Y. H. Tan⁶⁵, Y. X. Tan^{60,48}, C. J. Tang⁴⁵, G. Y. Tang¹, J. Tang⁴⁹, V. Thoren⁶⁴, B. Tsednee²⁶, I. Uman^{51D}, B. Wang¹, B. L. Wang⁵², C. W. Wang³⁶, D. Y. Wang^{38,k}, H. P. Wang^{1,52}, K. Wang^{1,48}, L. L. Wang¹, M. Wang⁴¹, M. Z. Wang^{38,k}, Meng Wang^{1,52}, W. H. Wang⁶⁵, W. P. Wang^{60,48}, X. Wang^{38,k}, X. F. Wang³², X. L. Wang^{9,h}, Y. Wang⁴⁹, Y. Wang^{60,48}, Y. D. Wang¹⁵, Y. F. Wang^{1,48,52}, Y. Q. Wang¹, Z. Wang^{1,48}, Z. Y. Wang¹, Ziyi Wang⁵², Zongyuan Wang^{1,52}, D. H. Wei¹², P. Weidenkaff²⁸, F. Weidner⁵⁷, S. P. Wen¹, D. J. White⁵⁵, U. Wiedner⁴, G. Wilkinson⁵⁸, M. Wolke⁶⁴, L. Wollenberg⁴, J. F. Wu^{1,52}, L. H. Wu¹, L. J. Wu^{1,52}, X. Wu^{9,h}, Z. Wu^{1,48}, L. Xia^{60,48}, H. Xiao^{9,h}, S. Y. Xiao¹, Y. J. Xiao^{1,52}, Z. J. Xiao³⁵, X. H. Xie^{38,k}, Y. G. Xie^{1,48}, Y. H. Xie⁶, T. Y. Xing^{1,52}, X. A. Xiong^{1,52}, G. F. Xu¹, J. J. Xu³⁶, Q. J. Xu¹⁴, W. Xu^{1,52}, X. P. Xu⁴⁶, L. Yan^{9,h}, L. Yan^{63A,63C}, W. B. Yan^{60,48}, W. C. Yan⁶⁸, Xu Yan⁴⁶, H. J. Yang^{42,g}, H. X. Yang¹, L. Yang⁶⁵, R. X. Yang^{60,48}, S. L. Yang^{1,52}, Y. H. Yang³⁶, Y. X. Yang¹², Yifan Yang^{1,52}, Zhi Yang²⁵, M. Ye^{1,48}, M. H. Ye⁷, J. H. Yin¹, Z. Y. You⁴⁹,

B. X. Yu^{1,48,52}, C. X. Yu³⁷, G. Yu^{1,52}, J. S. Yu^{20,l}, T. Yu⁶¹, C. Z. Yuan^{1,52}, W. Yuan^{63A,63C}, X. Q. Yuan^{38,k}, Y. Yuan¹, Z. Y. Yuan⁴⁹, C. X. Yue³³, A. Yuncu^{51B,a}, A. A. Zafar⁶², Y. Zeng^{20,l}, B. X. Zhang¹, Guangyi Zhang¹⁶, H. H. Zhang⁴⁹, H. Y. Zhang^{1,48}, J. L. Zhang⁶⁶, J. Q. Zhang⁴, J. W. Zhang^{1,48,52}, J. Y. Zhang¹, J. Z. Zhang^{1,52}, Jianyu Zhang^{1,52}, Jiawei Zhang^{1,52}, L. Zhang¹, Lei Zhang³⁶, S. Zhang⁴⁹, S. F. Zhang³⁶, T. J. Zhang^{42,g}, X. Y. Zhang⁴¹, Y. Zhang⁵⁸, Y. H. Zhang^{1,48}, Y. T. Zhang^{60,48}, Yan Zhang^{60,48}, Yao Zhang¹, Yi Zhang^{9,h}, Z. H. Zhang⁶, Z. Y. Zhang⁶⁵, G. Zhao¹, J. Zhao³³, J. Y. Zhao^{1,52}, J. Z. Zhao^{1,48}, Lei Zhao^{60,48}, Ling Zhao¹, M. G. Zhao³⁷, Q. Zhao¹, S. J. Zhao⁶⁸, Y. B. Zhao^{1,48}, Y. X. Zhao Zhao²⁵, Z. G. Zhao^{60,48}, A. Zhemchugov^{29,b}, B. Zheng⁶¹, J. P. Zheng^{1,48}, Y. Zheng^{38,k}, Y. H. Zheng⁵², B. Zhong³⁵, C. Zhong⁶¹, L. P. Zhou^{1,52}, Q. Zhou^{1,52}, X. Zhou⁶⁵, X. K. Zhou⁵², X. R. Zhou^{60,48}, A. N. Zhu^{1,52}, J. Zhu³⁷, K. Zhu¹, K. J. Zhu^{1,48,52}, S. H. Zhu⁵⁹, W. J. Zhu³⁷, X. L. Zhu⁵⁰, Y. C. Zhu^{60,48}, Z. A. Zhu^{1,52}, B. S. Zou¹, J. H. Zou¹

(BESIII Collaboration)

¹ Institute of High Energy Physics, Beijing 100049, People's Republic of China

² Beihang University, Beijing 100191, People's Republic of China

³ Beijing Institute of Petrochemical Technology, Beijing 102617, People's Republic of China

⁴ Bochum Ruhr-University, D-44780 Bochum, Germany

⁵ Carnegie Mellon University, Pittsburgh, Pennsylvania 15213, USA

⁶ Central China Normal University, Wuhan 430079, People's Republic of China

⁷ China Center of Advanced Science and Technology, Beijing 100190, People's Republic of China

⁸ COMSATS University Islamabad, Lahore Campus, Defence Road, Off Raiwind Road, 54000 Lahore, Pakistan

⁹ Fudan University, Shanghai 200443, People's Republic of China

¹⁰ G.I. Budker Institute of Nuclear Physics SB RAS (BINP), Novosibirsk 630090, Russia

¹¹ GSI Helmholtzcentre for Heavy Ion Research GmbH, D-64291 Darmstadt, Germany

¹² Guangxi Normal University, Guilin 541004, People's Republic of China

¹³ Guangxi University, Nanning 530004, People's Republic of China

¹⁴ Hangzhou Normal University, Hangzhou 310036, People's Republic of China

¹⁵ Helmholtz Institute Mainz, Johann-Joachim-Becher-Weg 45, D-55099 Mainz, Germany

¹⁶ Henan Normal University, Xinxiang 453007, People's Republic of China

¹⁷ Henan University of Science and Technology, Luoyang 471003, People's Republic of China

¹⁸ Huangshan College, Huangshan 245000, People's Republic of China

¹⁹ Hunan Normal University, Changsha 410081, People's Republic of China

²⁰ Hunan University, Changsha 410082, People's Republic of China

²¹ Indian Institute of Technology Madras, Chennai 600036, India

²² Indiana University, Bloomington, Indiana 47405, USA

²³ (A)INFN Laboratori Nazionali di Frascati, I-00044, Frascati,

Italy; (B)INFN and University of Perugia, I-06100, Perugia, Italy

²⁴ (A)INFN Sezione di Ferrara, I-44122, Ferrara, Italy; (B)University of Ferrara, I-44122, Ferrara, Italy

²⁵ Institute of Modern Physics, Lanzhou 730000, People's Republic of China

²⁶ Institute of Physics and Technology, Peace Ave. 54B, Ulaanbaatar 13330, Mongolia

²⁷ Jilin University, Changchun 130012, People's Republic of China

²⁸ Johannes Gutenberg University of Mainz, Johann-Joachim-Becher-Weg 45, D-55099 Mainz, Germany

²⁹ Joint Institute for Nuclear Research, 141980 Dubna, Moscow region, Russia

³⁰ Justus-Liebig-Universitaet Giessen, II. Physikalisches Institut, Heinrich-Buff-Ring 16, D-35392 Giessen, Germany

³¹ KVI-CART, University of Groningen, NL-9747 AA Groningen, The Netherlands

³² Lanzhou University, Lanzhou 730000, People's Republic of China

³³ Liaoning Normal University, Dalian 116029, People's Republic of China

³⁴ Liaoning University, Shenyang 110036, People's Republic of China

³⁵ Nanjing Normal University, Nanjing 210023, People's Republic of China

³⁶ Nanjing University, Nanjing 210093, People's Republic of China

³⁷ Nankai University, Tianjin 300071, People's Republic of China

³⁸ Peking University, Beijing 100871, People's Republic of China

³⁹ Qufu Normal University, Qufu 273165, People's Republic of China

⁴⁰ Shandong Normal University, Jinan 250014, People's Republic of China

- ⁴¹ Shandong University, Jinan 250100, People's Republic of China
⁴² Shanghai Jiao Tong University, Shanghai 200240, People's Republic of China
⁴³ Shanxi Normal University, Linfen 041004, People's Republic of China
⁴⁴ Shanxi University, Taiyuan 030006, People's Republic of China
⁴⁵ Sichuan University, Chengdu 610064, People's Republic of China
⁴⁶ Soochow University, Suzhou 215006, People's Republic of China
⁴⁷ Southeast University, Nanjing 211100, People's Republic of China
⁴⁸ State Key Laboratory of Particle Detection and Electronics, Beijing 100049, Hefei 230026, People's Republic of China
⁴⁹ Sun Yat-Sen University, Guangzhou 510275, People's Republic of China
⁵⁰ Tsinghua University, Beijing 100084, People's Republic of China
⁵¹ (A)Ankara University, 06100 Tandoğan, Ankara, Turkey; (B)Istanbul Bilgi University, 34060 Eyüp, İstanbul, Turkey;
(C)Uludag University, 16059 Bursa, Turkey; (D)Near East University, Nicosia, North Cyprus, Mersin 10, Turkey
⁵² University of Chinese Academy of Sciences, Beijing 100049, People's Republic of China
⁵³ University of Hawaii, Honolulu, Hawaii 96822, USA
⁵⁴ University of Jinan, Jinan 250022, People's Republic of China
⁵⁵ University of Manchester, Oxford Road, Manchester, M13 9PL, United Kingdom
⁵⁶ University of Minnesota, Minneapolis, Minnesota 55455, USA
⁵⁷ University of Muenster, Wilhelm-Klemm-Str. 9, 48149 Muenster, Germany
⁵⁸ University of Oxford, Keble Rd, Oxford, UK OX13RH
⁵⁹ University of Science and Technology Liaoning, Anshan 114051, People's Republic of China
⁶⁰ University of Science and Technology of China, Hefei 230026, People's Republic of China
⁶¹ University of South China, Hengyang 421001, People's Republic of China
⁶² University of the Punjab, Lahore-54590, Pakistan
⁶³ (A)University of Turin, I-10125, Turin, Italy; (B)University of Eastern Piedmont, I-15121, Alessandria, Italy; (C)INFN, I-10125, Turin, Italy
⁶⁴ Uppsala University, Box 516, SE-75120 Uppsala, Sweden
⁶⁵ Wuhan University, Wuhan 430072, People's Republic of China
⁶⁶ Xinyang Normal University, Xinyang 464000, People's Republic of China
⁶⁷ Zhejiang University, Hangzhou 310027, People's Republic of China
⁶⁸ Zhengzhou University, Zhengzhou 450001, People's Republic of China
- ^a Also at Bogazici University, 34342 Istanbul, Turkey
^b Also at the Moscow Institute of Physics and Technology, Moscow 141700, Russia
^c Also at the Novosibirsk State University, Novosibirsk, 630090, Russia
^d Also at the NRC "Kurchatov Institute", PNPI, 188300, Gatchina, Russia
^e Also at Istanbul Arel University, 34295 Istanbul, Turkey
^f Also at Goethe University Frankfurt, 60323 Frankfurt am Main, Germany
- ^g Also at Key Laboratory for Particle Physics, Astrophysics and Cosmology, Ministry of Education; Shanghai Key Laboratory for Particle Physics and Cosmology; Institute of Nuclear and Particle Physics, Shanghai 200240, People's Republic of China
^h Also at Key Laboratory of Nuclear Physics and Ion-beam Application (MOE) and Institute of Modern Physics, Fudan University, Shanghai 200443, People's Republic of China
ⁱ Also at Harvard University, Department of Physics, Cambridge, MA, 02138, USA
^j Currently at: Institute of Physics and Technology, Peace Ave.54B, Ulaanbaatar 13330, Mongolia
^k Also at State Key Laboratory of Nuclear Physics and Technology, Peking University, Beijing 100871, People's Republic of China
^l School of Physics and Electronics, Hunan University, Changsha 410082, China

(Dated: February 12, 2021)

We present an analysis of the process $\psi(3686) \rightarrow \Omega^- \bar{\Omega}^+$ ($\Omega^- \rightarrow K^- \Lambda$, $\bar{\Omega}^+ \rightarrow K^+ \bar{\Lambda}$, $\Lambda \rightarrow p \pi^-$, $\bar{\Lambda} \rightarrow \bar{p} \pi^+$) based on a data set of 448×10^6 $\psi(3686)$ decays collected with the BESIII detector at the BEPCII electron-positron collider. The helicity amplitudes for the process $\psi(3686) \rightarrow \Omega^- \bar{\Omega}^+$ and the decay parameters of the subsequent decay $\Omega^- \rightarrow K^- \Lambda$ ($\bar{\Omega}^+ \rightarrow K^+ \bar{\Lambda}$) are measured for the first time by a fit to the angular distribution of the complete decay chain, and the spin of the Ω^- is determined to be 3/2 for the first time since its discovery more than 50 years before.

The discovery of the Ω^- [1] was a crucial step in our understanding of the microcosmos. It was a great triumph for the eight-fold way model of baryons [2] and it led to the postulate of color charge [3]. A key feature of the eight-fold way and the quark model is that the Ω^- spin is $J = 3/2$, a prediction that has never been unambiguously confirmed by experiment. The current best determination of $J = 3/2$ is based on an analysis [4] that assumes the spins of both the Ξ_c^0 and the Ω_c^0 are their quark model values of $J = 1/2$.

One of the conceptually simplest processes in which a baryon-antibaryon pair can be created is electron-positron annihilation. In this Letter, two Ω^- spin hypotheses, $J = 1/2$ or $J = 3/2$, are tested using the joint angular distribution of the sequential decays of $e^+e^- \rightarrow \Omega^-\bar{\Omega}^+$ process. For $J = 1/2$ hypothesis, two form factors are needed in the production of baryon-antibaryon pair in electron-positron annihilation, a clear vector polarization, strongly dependent on the baryon direction is observed [5, 6]. For $J = 3/2$ hypothesis, the annihilation process involves four complex form factors [7]. In addition to vector polarization, the spin-3/2 fermions can have quadrupole and octupole polarization [8, 9]. Polarization of the Ω^- can be studied using the chain of weak decays $\Omega^- \rightarrow K^-\Lambda$ and $\Lambda \rightarrow p\pi^-$, where the first decay is described by the ratio α_{Ω^-} and the relative phase ϕ_{Ω^-} between the parity-conserving P -wave and parity-violating D -wave (S -wave for $J = 1/2$ hypothesis) decay amplitudes. The decay parameters cannot be calculated reliably in theory [11–13] and only α_{Ω^-} has been previously measured [14–16].

The resonance production process $e^+e^- \rightarrow \psi(3686) \rightarrow \Omega^-\bar{\Omega}^+$ was observed by the CLEO-c experiment with 27 ± 5 and 326 ± 19 events using the double-tag and single-tag technique as described in Refs. [17] and [18], respectively. With the world's largest $\psi(3686)$ data sample of $(448.1 \pm 2.9) \times 10^6$ $\psi(3686)$ events accumulated in e^+e^- annihilation with BESIII detector [19], we are able to select about 4000 $\psi(3686) \rightarrow \Omega^-\bar{\Omega}^+$ events, and establish for the first time that the Ω^- spin is $J = 3/2$ and measure Ω^- polarizations in the $\psi(3686) \rightarrow \Omega^-\bar{\Omega}^+$ reaction, and evidence for the dominance of the parity violating D -wave amplitude in the weak decay $\Omega^- \rightarrow K^-\Lambda$.

For the $J = 3/2$ hypothesis, in helicity formalism [20, 21], there are four helicity amplitudes in the production density matrix for $e^+e^- \rightarrow \psi(3686) \rightarrow \Omega^-\bar{\Omega}^+$ [10]. We define the ratios $A_{\frac{1}{2},\frac{1}{2}}/A_{\frac{1}{2},-\frac{1}{2}} = h_1 e^{i\phi_1}$, $A_{\frac{3}{2},\frac{1}{2}}/A_{\frac{1}{2},-\frac{1}{2}} = h_3 e^{i\phi_3}$, $A_{\frac{3}{2},\frac{3}{2}}/A_{\frac{1}{2},-\frac{1}{2}} = h_4 e^{i\phi_4}$, where, h_i and ϕ_i ($i = 1, 3, 4$) are real numbers to be determined from fits to data samples. The angular distribution is given by the trace of the Ω^- spin density matrix [10]: $1 + \alpha_{\psi(3686)} \cos^2 \theta_{\Omega^-}$, where $\alpha_{\psi(3686)} = (1 - 2(|h_1|^2 - |h_3|^2 + |h_4|^2))/(1 + 2(|h_1|^2 + |h_3|^2 + |h_4|^2))$. When considering the weak decays $\Omega^- \rightarrow K^-\Lambda$ and $\Lambda \rightarrow p\pi^-$, additional parameters α_{Ω^-} , α_Λ and ϕ_{Ω^-} describing the ratio and relative phase between two helicity amplitudes are needed [10]. The joint angular distribution of θ_{Ω^-} , θ_Λ , ϕ_Λ , θ_p and ϕ_p (see Fig. 1) is [10]

$$\rho_{3/2} = \sum_{\mu=0}^{15} \sum_{\nu=0}^3 r_\mu b_{\mu\nu} a_{\nu 0}. \quad (1)$$

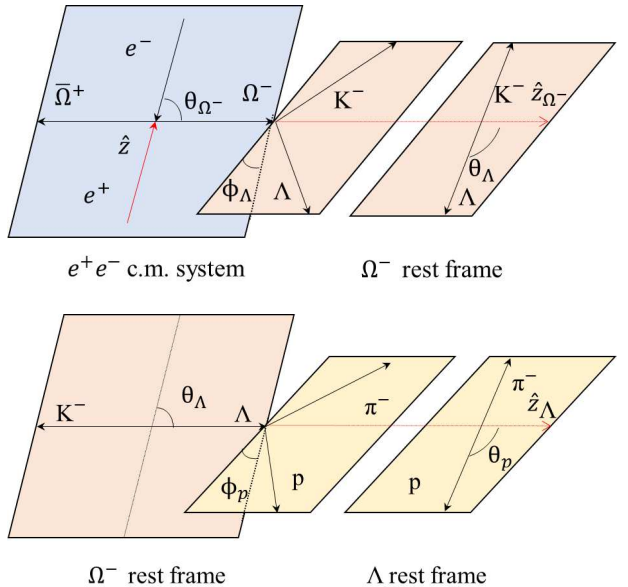


FIG. 1. Definition of the helicity angles used in the analysis. The helicity angles θ_{Ω^-} , θ_Λ , ϕ_Λ , θ_p and ϕ_p are spherical coordinates of the Ω^- , Λ and p momenta in three reference frames: the e^+e^- c.m. system and the Ω^- and Λ rest frames, respectively. The \hat{z} -axis in the e^+e^- c.m. system points along the incoming positron and \hat{z}_{Ω^-} is the Ω^- momentum direction. The polar axis direction in the Ω^- rest frame is \hat{z}_{Ω^-} and \hat{y}_{Ω^-} is along $\hat{z} \times \hat{z}_{\Omega^-}$, where \hat{z}_Λ is the Λ momentum direction. The polar axis direction in the Λ rest frame is \hat{z}_Λ and \hat{y}_Λ is along $\hat{z}_{\Omega^-} \times \hat{z}_\Lambda$.

For the $J = 1/2$ hypothesis, the joint angular distribution is defined as [10]:

$$\rho_{1/2} = \sum_{\mu=0}^3 \sum_{\nu=0}^3 r_\mu a_{\mu\nu} a_{\nu 0}. \quad (2)$$

Here r_μ , $b_{\mu\nu}/a_{\mu\nu}$, and $a_{\nu 0}$ are defined in terms of the helicity amplitudes [10]. By fitting the joint angular distribution of the selected events with Eqs. (1) and (2), we can in principle obtain the helicity amplitudes and Ω^-/Λ decay parameters.

To maximize the reconstruction efficiency, a single-tag method is implemented in which only the Ω^- or the $\bar{\Omega}^+$ is reconstructed via $\Omega^- \rightarrow K^-\Lambda \rightarrow K^-\pi^-$ or $\bar{\Omega}^+ \rightarrow K^+\bar{\Lambda} \rightarrow K^+\bar{p}\pi^+$, and the $\bar{\Omega}^+$ or Ω^- on the recoil side is inferred from the missing mass of the reconstructed particles. The following event selections are described for $\Omega^- \rightarrow K^-\pi^-$ as an example, the same selections are also applied for the $\bar{\Omega}^+$ selection.

Charged tracks reconstructed from multilayer drift chamber (MDC) hits are required to be within a polar-angle (θ) range of $|\cos \theta| < 0.93$. To determine the species of final-state particles, specific energy loss (dE/dx) information is used to form particle identification (PID) probabilities for pion, kaon, and proton hypotheses. Charged particles are identified as the hypothesis with the highest probability and only one K^- and one proton are required in each event. The rest of the negative charged tracks in an event are assumed to be π^- . To avoid potentially large differences between data and Monte

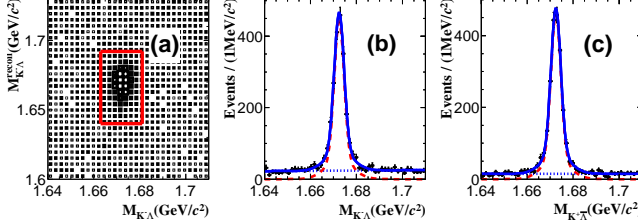


FIG. 2. (a) Distribution of $M_{K-\Lambda}^{\text{recoil}}$ versus $M_{K-\Lambda}$ of the selected $K-\Lambda$ candidates in Ω^- reconstruction process. The red solid box shows the signal region of $\psi(3686) \rightarrow \Omega^- \bar{\Omega}^+$. (b) Projection onto $M_{K-\Lambda}$ for events with $M_{K-\Lambda}^{\text{recoil}}$ in signal region. (c) Same as (b) but for $K^+\bar{\Lambda}$ tagged events. Dots with error bars are data, the solid blue curves show the results of the fit, the red dashed lines show the signal components of the fit, and the blue dotted lines show the background components of the fit.

Carlo (MC) simulation for very low momentum tracks, the transverse momenta of the p , K^- , and π^- tracks are required to be larger than 0.2, 0.1, and 0.05 GeV/c , respectively.

The $\Lambda \rightarrow p\pi^-$ candidates are reconstructed by applying a vertex fit to the identified proton and a negatively charged pion with an invariant mass ($M_{p\pi^-}$) in the mass window of [1.110, 1.122] GeV/c^2 . If more than one Λ candidate is found, the one with $p\pi^-$ invariant mass closest to the nominal Λ mass [22] is kept. The Λ candidate is then combined with a K^- track to reconstruct the Ω^- . A secondary vertex fit is applied to $K^-\Lambda$ to improve the Ω^- -mass resolution and to suppress backgrounds. The invariant mass of $K^-\Lambda$ ($M_{K-\Lambda}$) is requirement in the mass window of [1.663, 1.681] GeV/c^2 . To obtain the antibaryon candidates $\bar{\Omega}^+$, we require the recoiling mass of $K^-\Lambda$ ($M_{K-\Lambda}^{\text{recoil}}$) in the mass window of [1.640, 1.692] GeV/c^2 . All the mass windows are determined by optimizing the figure of merit $\frac{s}{\sqrt{s+b}}$ with s being the number of signal events expected in data and b the number of the backgrounds in data estimated by using a normalization factor of sideband regions and signal region.

The distribution of $M_{K-\Lambda}$ vs. $M_{K-\Lambda}^{\text{recoil}}$ of the selected $K-\Lambda$ candidates is shown in Fig. 2(a). A clear cluster of events in the data sample corresponding to $\psi(3686) \rightarrow \Omega^- \bar{\Omega}^+$ is observed in the signal region of red box area.

An inclusive $\psi(3686)$ MC sample with 4×10^8 $\psi(3686)$ events is used to study the possible background sources [23] included in the simulation, and no peaking background is found. The continuum production of $\Omega^- \bar{\Omega}^+$ is expected to be very low and neglected. This is also checked with data collected at 3.65 GeV with an integrated luminosity of 49 pb^{-1} (about 7% of the $\psi(3686)$ data sample), no significant $\Omega^- \bar{\Omega}^+$ signal is observed.

Events in the signal region, shown in Fig. 2(a), are used to perform the angular distribution analysis. After applying all the event selections, 2507 $\psi(3686) \rightarrow \Omega^- \bar{\Omega}^+$ candidates are selected by tagging the Ω^- (called the Ω^- sample), and 2238 candidates by tagging the $\bar{\Omega}^+$ (called

the $\bar{\Omega}^+$ sample) by counting. The number of non- Ω^- background events is estimated from the numbers of events in the Ω^- -mass sideband as $M_{K-\Lambda} \in [1.644, 1.653]$ or $[1.692, 1.701]$ GeV/c^2 . The Ω^- ($\bar{\Omega}^+$) sample is estimated to contain 298 ± 17 (189 ± 14) background events.

An unbinned maximum likelihood fit to the selected events is performed to measure the free parameters in the angular distribution. The likelihood function is defined as

$$\mathcal{L} = \prod_{j=1}^{N_t} W(\zeta_j | H) = \prod_{j=1}^{N_t} \frac{\rho(\zeta_j | H) \times \epsilon(\zeta_j)}{N(H)}, \quad (3)$$

where j is the candidate event number, $\rho(\zeta_j | H)$ is the angular distribution function for the cascade decay in Eqs. (1) and (2), $\zeta = \{\theta_\Omega, \theta_\Lambda, \phi_\Lambda, \theta_p, \phi_p\}$ are the angular distribution variables, and H contains the parameters to be determined from the fit. N_t is the number of the selected events in the data samples. $N(H)$ is the normalization factor calculated with the MC integration method, and $\epsilon(\zeta_j)$ is the detection efficiency. Contributions from the background events to the likelihood have been considered by using events in the sideband regions of the Ω^- . The fit is performed by minimizing the objective function $S = -(\ln \mathcal{L}_{\text{data}} - \ln \mathcal{L}_{\text{bg}})$, where $\mathcal{L}_{\text{data}}$ is the likelihood function of events selected in the signal region of Ω^- and $\bar{\Omega}^+$ samples, and \mathcal{L}_{bg} is the likelihood function of background events of these two single-tag samples estimated by the sideband method.

The decay parameters α_Λ and α_{Ω^-} are fixed to the PDG averages of previously measured values [5, 14–16]. Assuming that there is no CP -violation in Ω^- and Λ decays, $\alpha_\Lambda = -\alpha_{\bar{\Lambda}} = 0.753 \pm 0.007$ and $\alpha_{\Omega^-} = -\alpha_{\bar{\Omega}^+} = 0.0154 \pm 0.0017$ [24]. A simultaneous fit is performed to the Ω^- and $\bar{\Omega}^+$ events selected from data in which the constraint $\phi_{\Omega^-} = -\phi_{\bar{\Omega}^+}$ is applied. The change of $2S$ of the fit assuming $J = 1/2$ and that of a linear combination of $J = 1/2$ and $J = 3/2$ is -232 with 8 more free parameters, so we determine the significance of the $J = 3/2$ hypothesis over the $J = 1/2$ to be larger than 14σ , thus determine the spin of Ω^- as $3/2$ unambiguously. For the fit with $J = 3/2$, we find two solutions with identical fit quality, as shown in Table I. Tests with large MC sample confirm the existence of two solutions in such fits although its origin is not obvious in the expression of the decay amplitude. The statistical and systematic covariance matrices for the two solutions are supplied in the Supplemental Material.

The signal MC events generated with PHSP are weighted with matrix elements calculated with the parameters obtained from the fits and the weighted MC sample predictions are compared with data in five distributions of the helicity angle, with the background contributions estimated from the Ω^- sideband regions indicated as green histogram. We observe that the fit with Ω^- spin $J = 3/2$ describes data very well while $J = 1/2$ fails to describe data, as shown in Fig. 3(a) for $\cos \theta_{\Lambda/\bar{\Lambda}}$, which has the most prominent difference. The moments M_6 and M_8 defined as $M_\mu = \frac{1}{N} \sum_{j=0}^N \sum_{k=0}^3 b_{\mu,\kappa} a_{\kappa,0}$ are compared between data and those two weighted MC samples, as shown in Figs. 3

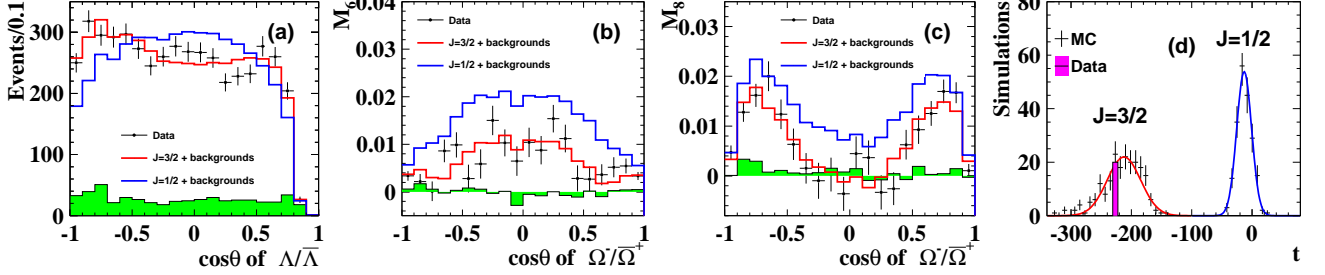


FIG. 3. (a) The $\cos\theta_{\Lambda/\bar{\Lambda}}$ distributions of data (dots with error bars) and fits with $J = 3/2$ (red histogram) and $J = 1/2$ (blue histogram) hypotheses; (b) and (c) are the M_6 and M_8 distributions of data and fit results; and (d) distribution of the test statistic $t = S^{J=1/2} - S^{J=3/2}$ for a series of MC simulations performed under the $J = 1/2$ (right peak) and $J = 3/2$ (left peak) hypotheses. The lines represent Gaussian fits to the simulated data points. The t value obtained from experimental data is indicated by the vertical bar.

TABLE I. Two sets of fit values of the helicity parameters in $\psi(3686) \rightarrow \Omega^-\bar{\Omega}^+$ decays of spin-3/2 hypothesis. The first uncertainties are statistical, and the second ones systematic.

parameter	solution I	solution II
h_1	$0.30 \pm 0.11 \pm 0.04$	$0.31 \pm 0.10 \pm 0.04$
ϕ_1	$0.69 \pm 0.41 \pm 0.13$	$2.38 \pm 0.37 \pm 0.13$
h_3	$0.26 \pm 0.05 \pm 0.02$	$0.27 \pm 0.05 \pm 0.01$
ϕ_3	$2.60 \pm 0.16 \pm 0.08$	$2.57 \pm 0.16 \pm 0.04$
h_4	$0.51 \pm 0.03 \pm 0.01$	$0.51 \pm 0.03 \pm 0.01$
ϕ_4	$0.34 \pm 0.80 \pm 0.31$	$1.37 \pm 0.68 \pm 0.16$
ϕ_Ω	$4.29 \pm 0.45 \pm 0.23$	$4.15 \pm 0.44 \pm 0.16$

(b) and (c). Here N is the number of events in the data or MC samples. Clear preference of $J = 3/2$ over $J = 1/2$ is observed. Since the two sets of solutions describe the data equally well, we only show the angular distributions for one set of them.

The likelihood ratio $t = 2(S^{J=1/2} - S^{J=3/2})$ is used as a test variable to discriminate between the $J = 3/2$ and $J = 1/2$ hypotheses [25]. The MC sample for each hypothesis is generated according to its joint angular distribution, propagated through the detector model and subjected to the same event selection criteria as the experimental data. Each MC subset has the same size as the real data samples and is assumed to have the same amount of background. The test statistic t distribution is shown in Fig. 3(d). The simulations for the right peak were performed under the $J = 1/2$ hypothesis, while those in the left peak correspond to the $J = 3/2$ hypothesis. It is clear that the t distributions of the two hypotheses are well separated. Since the t -value from the data lies well within the left peak, our data favour the $J = 3/2$ hypothesis.

The following systematic uncertainties are considered for the angular distribution measurement. The tracking and PID efficiencies are studied with control samples of $J/\psi \rightarrow p\bar{p}\pi^+\pi^-$, $J/\psi \rightarrow \Lambda\bar{\Lambda}$ ($\Lambda \rightarrow p\pi^-$, $\bar{\Lambda} \rightarrow \bar{p}\pi^+$), $J/\psi \rightarrow K_SK^-\pi^+ + c.c.$, and $J/\psi \rightarrow pK^-\bar{\Lambda} + c.c.$, and the polar angle and transverse momentum (p_t) dependent efficiencies are measured. Subsequently, the efficiency of MC events is corrected by the two-dimensional efficiency

TABLE II. Summary of the systematic uncertainties for the decay parameters in solution I (solution II) of $\psi(3686) \rightarrow \Omega^-\bar{\Omega}^+$.

	track/PID	background	α_Λ	total
Δh_1	$0.04(0.04)$	$0(0.01)$	$0(0)$	$0.04(0.04)$
$\Delta \phi_1$	$0.13(0.12)$	$0.02(0.04)$	$0.01(0.01)$	$0.13(0.13)$
Δh_3	$0.01(0.01)$	$0(0)$	$0.02(0)$	$0.02(0.01)$
$\Delta \phi_3$	$0.03(0.03)$	$0.07(0.02)$	$0(0.01)$	$0.08(0.04)$
Δh_4	$0.01(0.01)$	$0(0.01)$	$0(0)$	$0.01(0.01)$
$\Delta \phi_4$	$0.28(0.11)$	$0.13(0.12)$	$0.02(0)$	$0.31(0.16)$
$\Delta \phi_\Omega$	$0.16(0.16)$	$0.17(0.03)$	$0(0.01)$	$0.23(0.16)$

scale factors and the uncertainty is estimated by varying the efficiency scale factors by one standard deviation for each p_t vs. $\cos\theta$ bin. The differences between the new fit results and the nominal ones are taken as the systematic uncertainties. The uncertainty due to the background estimation is estimated by changing the Ω^- -sideband regions from $[1.644, 1.653]$ and $[1.692, 1.701]$ GeV/ c^2 to $[1.643, 1.653]$ and $[1.692, 1.702]$ GeV/ c^2 . The differences between fit results with and without changing sideband regions are taken as the systematic uncertainties. The uncertainties arising from the values of the fixed parameters α_{Ω^-} and α_Λ are estimated by changing these two parameters by one standard deviation separately, then comparing the refitted parameters with the original results. We find that the uncertainty of α_{Ω^-} can be neglected. All of the above contributions are added in quadrature to obtain the total systematic uncertainties as shown in Table II.

From Table I we find that the magnitudes of the amplitudes are about the same in the two solutions while the phases ϕ_1 and ϕ_4 can be very different. All the h_i values are less than one, which means that the amplitude $A_{\frac{1}{2}, -\frac{1}{2}}$ dominates the decay process. The value of ϕ_{Ω^-} provides information on whether the process is P -wave dominant ($\phi_{\Omega^-} = 0$) or D -wave dominant ($\phi_{\Omega^-} = \pi$). By comparing the maximum-likelihood values between the fit with ϕ_{Ω^-} fixed to zero or π and the nominal fit, we find that the significance for non-zero ϕ_{Ω^-} is 3.7σ and that for a non- π ϕ_{Ω^-} is 1.5σ . Thus, ϕ_{Ω^-} favours the D -wave dominant case, which differs from the theoretical predictions of P -wave dominance [26]. The ratio

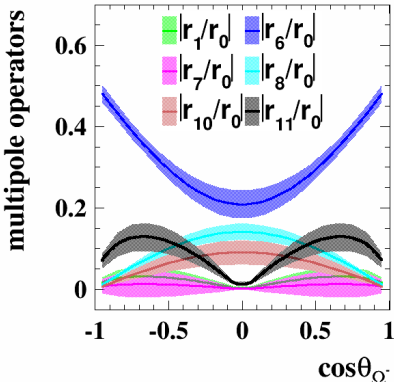


FIG. 4. The $\cos \theta_{\Omega^-}$ dependence of the multipolar polarization operators. The solid lines represent the central values, and the shaded areas represent \pm one standard deviation.

of D - to P -wave can be calculated as $|A_D|^2/|A_P|^2 = 2.4 \pm 2.0$ (solution I), and $|A_D|^2/|A_P|^2 = 3.3 \pm 2.9$ (solution II), where the uncertainty is the sum in quadrature of the statistical and systematic uncertainties. Allowing α_{Ω^-} to be determined by the fit, we obtain $\alpha_{\Omega^-} = -0.04 \pm 0.03$, which does not contradict with the quoted result from previous experiments but with poorer precision [14–16].

To conclude, based on 448×10^6 $\psi(3686)$ events, we observe 4035 ± 76 $\psi(3686) \rightarrow \Omega^- \bar{\Omega}^+$ signal events. We conduct the first study of the angular distribution of the three-stage decay, and found that the hypothesis of Ω^- has a spin of 3/2 is preferred over a spin of 1/2 with a significance of more than 14σ , and establishes the spin of the Ω^- to be 3/2 for the first time that is independent of any model-based assumptions. The helicity amplitudes of $\psi(3686) \rightarrow \Omega^- \bar{\Omega}^+$ and the decay parameter of $\Omega^- \rightarrow K^- \Lambda$, ϕ_{Ω^-} , are also measured for the first time. With the helicity amplitudes measured in Table I, $\alpha_{\psi(3686)} = 0.24 \pm 0.10$, where the uncertainty is the sum in quadrature of the statistical and systematic uncertainties.

With the helicity amplitudes measured in Table I, we calculate the $\cos \theta_{\Omega^-}$ dependence of the multipolar polarization operators as shown in Fig. 4. The uncertainties (statistical and systematic) are calculated using the covariance matrix of the fitted h_i and ϕ_i . For the process of $e^+ e^- \rightarrow \psi(3686) \rightarrow \Omega^- \bar{\Omega}^+$, Ω^- particles not only have vector polarization (r_1), but also have quadrupole (r_6, r_7, r_8) and octupole (r_{10}, r_{11}) polarization contributions [8, 9].

As a byproduct, with the same data sample, the branching fraction for $\psi(3686) \rightarrow \Omega^- \bar{\Omega}^+$ is measured as $(5.85 \pm 0.12 \pm 0.25) \times 10^{-5}$, where the first uncertainty is statistical systematic, and the second is systematic [27]. This result agrees with previous measurements [17, 18] with improved precision.

The BESIII collaboration thanks the staff of BEPCII and the IHEP computing center for their strong support. The authors would like to thank Prof. Zuo Tang Liang, Prof. Yukun Song, Prof. Xiaogang He, and Dr. Jusak Tandean for useful discussions. This work is supported in part by National

Key Basic Research Program of China under Contract No. 2020YFA0406300; National Natural Science Foundation of China (NSFC) under Contracts Nos. 11625523, 11635010, 11735014, 11822506, 11835012, 11935015, 11935016, 11935018, 11961141012; the Chinese Academy of Sciences (CAS) Large-Scale Scientific Facility Program; Joint Large-Scale Scientific Facility Funds of the NSFC and CAS under Contracts Nos. U1732263, U1832207; CAS Key Research Program of Frontier Sciences under Contracts Nos. QYZDJ-SSW-SLH003, QYZDJ-SSW-SLH040; 100 Talents Program of CAS; INPAC and Shanghai Key Laboratory for Particle Physics and Cosmology; ERC under Contract No. 758462; German Research Foundation DFG under Contracts Nos. 443159800, Collaborative Research Center CRC 1044, FOR 2359, GRK 214; Istituto Nazionale di Fisica Nucleare, Italy; Ministry of Development of Turkey under Contract No. DPT2006K-120470; National Science and Technology fund; Olle Engkvist Foundation under Contract No. 200-0605; STFC (United Kingdom); The Knut and Alice Wallenberg Foundation (Sweden) under Contract No. 2016.0157; The Royal Society, UK under Contracts Nos. DH140054, DH160214; The Swedish Research Council; U. S. Department of Energy under Contracts Nos. DE-FG02-05ER41374, DE-SC-0012069.

-
- [1] V. E. Barnes *et al.*, Phys. Rev. Lett. **12**, 204 (1964).
 - [2] M. Gell-Mann, Phys. Rev. **125**, 1067 (1962).
 - [3] O. W. Greenberg, Phys. Rev. Lett. **13**, 598 (1964).
 - [4] B. Aubert *et al.* (BaBar Collaboration), Phys. Rev. Lett. **97**, 112001 (2006).
 - [5] M. Ablikim *et al.* (BESIII Collaboration), Nature Phys. **15**, 631 (2019).
 - [6] M. Ablikim *et al.* (BESIII Collaboration), Phys. Rev. Lett. **123**, 122003 (2019).
 - [7] J. G. Korner and M. Kuroda, Phys. Rev. D **16**, 2165 (1977).
 - [8] M. G. Doncel, L. Michel and P. Minnaert, Nucl. Phys. B **38**, 477 (1972).
 - [9] A. Z. Dubnickova, S. Dubnicka and M. P. Rekalo, Nuovo Cim. A **109**, 241 (1996).
 - [10] E. Perotti, G. Fäldt, A. Kupsc, S. Leupold and J. J. Song, Phys. Rev. D **99**, 056008 (2019).
 - [11] M. Suzuki, Prog. Theor. Phys. **32**, 138 (1964).
 - [12] Y. Hara, Phys. Rev. **150**, 1175 (1966).
 - [13] J. Finjord, Phys. Lett. **76B**, 116 (1978).
 - [14] Y. C. Chen *et al.* (HyperCP Collaboration), Phys. Rev. D **71**, 051102 (2005).
 - [15] L. C. Lu *et al.* (HyperCP Collaboration), Phys. Lett. B **617**, 11 (2005).
 - [16] L. C. Lu *et al.* (HyperCP Collaboration), Phys. Rev. Lett. **96**, 242001 (2006).
 - [17] S. Dobbs, A. Tomaradze, T. Xiao, K. K. Seth and G. Bonvicini, Phys. Lett. B **739**, 90 (2014).
 - [18] S. Dobbs, K. K. Seth, A. Tomaradze, T. Xiao and G. Bonvicini, Phys. Rev. D **96**, 092004 (2017).
 - [19] M. Ablikim *et al.* (BESIII Collaboration), Nucl. Instrum. Meth. A **614**, 345 (2010).
 - [20] M. Jacob and G. C. Wick, Annals Phys. **7**, 404 (1959).

- [21] S. M. Berman and M. Jacob, Spin And Parity Analysis In Two Step Decay Processes, Tech. Rep. SLAC-43 (Stanford Linear Accelerator Center, 1965).
- [22] M. Tanabashi *et al.* (Particle Data Group), Phys. Rev. D **98**, 030001 (2018).
- [23] X. Zhou, S. Du, G. Li and C. Shen, Comput. Phys. Commun. **258**, 107540 (2021).
- [24] From the world average of $\alpha_{\Omega^-} \times \alpha_\Lambda = 0.0115 \pm 0.0013$ [14–16], by using the BESIII average of α_Λ and $\alpha_{\bar{\Lambda}}$ [5], $\alpha_\Lambda = 0.753 \pm 0.007$, we obtain $\alpha_{\Omega^-} = -\alpha_{\bar{\Omega}^+} = 0.0154 \pm 0.0017$.
- Here the uncertainties are combined statistical and systematic uncertainties, and CP symmetry is assumed in Λ and Ω decays.
- [25] R. Aaij *et al.* (LHCb Collaboration), Phys. Rev. D **92**, no. 1, 011102 (2015).
- [26] J. Tandean, Phys. Rev. D **70**, 076005 (2004).
- [27] See Supplemental Material [url] for brief description, which includes Refs. [28, 29].
- [28] R. G. Ping, Chin. Phys. C **32**, 599 (2008).
- [29] M. Ablikim *et al.* (BESIII Collaboration), Chin. Phys. C **42**, 023001 (2018).

Model independent determination of the spin of the Ω^- and its polarization alignment in $\psi(3686) \rightarrow \Omega^- \bar{\Omega}^+$

M. Ablikim¹, M. N. Achasov^{10,c}, P. Adlarson⁶⁴, S. Ahmed¹⁵, M. Albrecht⁴, A. Amoroso^{63A,63C}, Q. An^{60,48}, Anita²¹, Y. Bai⁴⁷, O. Bakina²⁹, R. Baldini Ferroli^{23A}, I. Balossino^{24A}, Y. Ban^{38,k}, K. Begzsuren²⁶, J. V. Bennett⁵, N. Berger²⁸, M. Bertani^{23A}, D. Bettone^{24A}, F. Bianchi^{63A,63C}, J. Biernat⁶⁴, J. Bloms⁵⁷, A. Bortone^{63A,63C}, I. Boyko²⁹, R. A. Briere⁵, H. Cai⁶⁵, X. Cai^{1,48}, A. Calcaterra^{23A}, G. F. Cao^{1,52}, N. Cao^{1,52}, S. A. Cetin^{51B}, J. F. Chang^{1,48}, W. L. Chang^{1,52}, G. Chelkov^{29,b}, D. Y. Chen⁶, G. Chen¹, H. S. Chen^{1,52}, M. L. Chen^{1,48}, S. J. Chen³⁶, X. R. Chen²⁵, Y. B. Chen^{1,48}, W. S. Cheng^{63C}, G. Cibinetto^{24A}, F. Cossio^{63C}, X. F. Cui³⁷, H. L. Dai^{1,48}, J. P. Dai^{42,g}, X. C. Dai^{1,52}, A. Dbeysi¹⁵, R. B. de Boer⁴, D. Dedovich²⁹, Z. Y. Deng¹, A. Denig²⁸, I. Denysenko²⁹, M. Destefanis^{63A,63C}, F. De Mori^{63A,63C}, Y. Ding³⁴, C. Dong³⁷, J. Dong^{1,48}, L. Y. Dong^{1,52}, M. Y. Dong^{1,48,52}, S. X. Du⁶⁸, J. Fang^{1,48}, S. S. Fang^{1,52}, Y. Fang¹, R. Farinelli^{24A}, L. Fava^{63B,63C}, F. Feldbauer⁴, G. Felici^{23A}, C. Q. Feng^{60,48}, M. Fritsch⁴, C. D. Fu¹, Y. Fu¹, X. L. Gao^{60,48}, Y. Gao⁶¹, Y. Gao^{38,k}, Y. G. Gao⁶, I. Garzia^{24A,24B}, E. M. Gersabeck⁵⁵, A. Gilman⁵⁶, K. Goetzen¹¹, L. Gong³⁷, W. X. Gong^{1,48}, W. Gradl²⁸, M. Greco^{63A,63C}, L. M. Gu³⁶, M. H. Gu^{1,48}, S. Gu², Y. T. Gu¹³, C. Y. Guan^{1,52}, A. Q. Guo²², L. B. Guo³⁵, R. P. Guo⁴⁰, Y. P. Guo²⁸, Y. P. Guo^{9,h}, A. Guskov²⁹, S. Han⁶⁵, T. T. Han⁴¹, T. Z. Han^{9,h}, X. Q. Hao¹⁶, F. A. Harris⁵³, K. L. He^{1,52}, F. H. Heinsius⁴, T. Held⁴, Y. K. Heng^{1,48,52}, M. Himmelreich^{11,f}, T. Holtmann⁴, Y. R. Hou⁵², Z. L. Hou¹, H. M. Hu^{1,52}, J. F. Hu^{42,g}, T. Hu^{1,48,52}, Y. Hu¹, G. S. Huang^{60,48}, L. Q. Huang⁶¹, X. T. Huang⁴¹, Z. Huang^{38,k}, N. Huesken⁵⁷, T. Hussain⁶², W. Ikegami Andersson⁶⁴, W. Imoehl²², M. Irshad^{60,48}, S. Jaeger⁴, S. Janchiv^{26,j}, Q. Ji¹, Q. P. Ji¹⁶, X. B. Ji^{1,52}, X. L. Ji^{1,48}, H. B. Jiang⁴¹, X. S. Jiang^{1,48,52}, X. Y. Jiang³⁷, J. B. Jiao⁴¹, Z. Jiao¹⁸, S. Jin³⁶, Y. Jin⁵⁴, T. Johansson⁶⁴, N. Kalantar-Nayestanaki³¹, X. S. Kang³⁴, R. Kappert³¹, M. Kavatsyuk³¹, B. C. Ke^{43,1}, I. K. Keshk⁴, A. Khoukaz⁵⁷, P. Kiese²⁸, R. Kiuchi¹, R. Kliemt¹¹, L. Koch³⁰, O. B. Kolcu^{51B,e}, B. Kopf⁴, M. Kuemmel⁴, M. Kuessner⁴, A. Kupsc⁶⁴, M. G. Kurth^{1,52}, W. Kühn³⁰, J. J. Lane⁵⁵, J. S. Lange³⁰, P. Larin¹⁵, L. Lavezzi^{63C}, H. Leithoff²⁸, M. Lellmann²⁸, T. Lenz²⁸, C. Li³⁹, C. H. Li³³, Cheng Li^{60,48}, D. M. Li⁶⁸, F. Li^{1,48}, G. Li¹, H. B. Li^{1,52}, H. J. Li^{9,h}, J. L. Li⁴¹, J. Q. Li⁴, Ke Li¹, L. K. Li¹, Lei Li³, P. L. Li^{60,48}, P. R. Li³², S. Y. Li⁵⁰, W. D. Li^{1,52}, W. G. Li¹, X. H. Li^{60,48}, X. L. Li⁴¹, Z. B. Li⁴⁹, Z. Y. Li⁴⁹, H. Liang^{60,48}, H. Liang^{1,52}, Y. F. Liang⁴⁵, Y. T. Liang²⁵, L. Z. Liao^{1,52}, J. Libby²¹, C. X. Lin⁴⁹, B. Liu^{42,g}, B. J. Liu¹, C. X. Liu¹, D. Liu^{60,48}, D. Y. Liu^{42,g}, F. H. Liu⁴⁴, Fang Liu¹, Feng Liu⁶, H. B. Liu¹³, H. M. Liu^{1,52}, Huanhuan Liu¹, Huihui Liu¹⁷, J. B. Liu^{60,48}, J. Y. Liu^{1,52}, K. Liu¹, K. Y. Liu³⁴, Ke Liu⁶, L. Liu^{60,48}, Q. Liu⁵², S. B. Liu^{60,48}, Shuai Liu⁴⁶, T. Liu^{1,52}, X. Liu³², Y. B. Liu³⁷, Z. A. Liu^{1,48,52}, Z. Q. Liu⁴¹, Y. F. Long^{38,k}, X. C. Lou^{1,48,52}, F. X. Lu¹⁶, H. J. Lu¹⁸, J. D. Lu^{1,52}, J. G. Lu^{1,48}, X. L. Lu¹, Y. Lu¹, Y. P. Lu^{1,48}, C. L. Luo³⁵, M. X. Luo⁶⁷, P. W. Luo⁴⁹, T. Luo^{9,h}, X. L. Luo^{1,48}, S. Lusso^{63C}, X. R. Lyu⁵², F. C. Ma³⁴, H. L. Ma¹, L. L. Ma⁴¹, M. M. Ma^{1,52}, Q. M. Ma¹, R. Q. Ma^{1,52}, R. T. Ma⁵², X. N. Ma³⁷, X. X. Ma^{1,52}, X. Y. Ma^{1,48}, Y. M. Ma⁴¹, F. E. Maas¹⁵, M. Maggiora^{63A,63C}, S. Maldaner²⁸, S. Malde⁵⁸, Q. A. Malik⁶², A. Mangoni^{23B}, Y. J. Mao^{38,k}, Z. P. Mao¹, S. Marcello^{63A,63C}, Z. X. Meng⁵⁴, J. G. Messchendorp³¹, G. Mezzadri^{24A}, T. J. Min³⁶, R. E. Mitchell²², X. H. Mo^{1,48,52}, Y. J. Mo⁶, N. Yu. Muchnoi^{10,c}, H. Muramatsu⁵⁶, S. Nakhoul^{11,f}, Y. Nefedov²⁹, F. Nerling^{11,f}, I. B. Nikolaev^{10,c}, Z. Ning^{1,48}, S. Nisar^{8,i}, S. L. Olsen⁵², Q. Ouyang^{1,48,52}, S. Pacetti^{23B}, X. Pan⁴⁶, Y. Pan⁵⁵, A. Pathak¹, P. Patteri^{23A}, M. Pelizaeus⁴, H. P. Peng^{60,48}, K. Peters^{11,f}, J. Pettersson⁶⁴, J. L. Ping³⁵, R. G. Ping^{1,52}, A. Pitka⁴, R. Poling⁵⁶, V. Prasad^{60,48}, H. Qi^{60,48}, H. R. Qi⁵⁰, M. Qi³⁶, T. Y. Qi², S. Qian^{1,48}, W.-B. Qian⁵², Z. Qian⁴⁹, C. F. Qiao⁵², L. Q. Qin¹², X. P. Qin¹³, X. S. Qin⁴, Z. H. Qin^{1,48}, J. F. Qiu¹, S. Q. Qu³⁷, K. H. Rashid⁶², K. Ravindran²¹, C. F. Redmer²⁸, A. Rivetti^{63C}, V. Rodin³¹, M. Rolo^{63C}, G. Rong^{1,52}, Ch. Rosner¹⁵, M. Rump⁵⁷, A. Sarantsev^{29,d}, Y. Schelhaas²⁸, C. Schnier⁴, K. Schoenning⁶⁴, D. C. Shan⁴⁶, W. Shan¹⁹, X. Y. Shan^{60,48}, M. Shao^{60,48}, C. P. Shen², P. X. Shen³⁷, X. Y. Shen^{1,52}, H. C. Shi^{60,48}, R. S. Shi^{1,52}, X. Shi^{1,48}, X. D. Shi^{60,48}, J. J. Song⁴¹, Q. Q. Song^{60,48}, W. M. Song²⁷, Y. X. Song^{38,k}, S. Sosio^{63A,63C}, S. Spataro^{63A,63C}, F. F. Sui⁴¹, G. X. Sun¹, J. F. Sun¹⁶, L. Sun⁶⁵, S. S. Sun^{1,52}, T. Sun^{1,52}, W. Y. Sun³⁵, Y. J. Sun^{60,48}, Y. K. Sun^{60,48}, Y. Z. Sun¹, Z. T. Sun¹, Y. H. Tan⁶⁵, Y. X. Tan^{60,48}, C. J. Tang⁴⁵, G. Y. Tang¹, J. Tang⁴⁹, V. Thoren⁶⁴, B. Tsednee²⁶, I. Uman^{51D}, B. Wang¹, B. L. Wang⁵², C. W. Wang³⁶, D. Y. Wang^{38,k}, H. P. Wang^{1,52}, K. Wang^{1,48}, L. L. Wang¹, M. Wang⁴¹, M. Z. Wang^{38,k}, Meng Wang^{1,52}, W. H. Wang⁶⁵, W. P. Wang^{60,48}, X. Wang^{38,k}, X. F. Wang³², X. L. Wang^{9,h}, Y. Wang⁴⁹, Y. Wang^{60,48}, Y. D. Wang¹⁵, Y. F. Wang^{1,48,52}, Y. Q. Wang¹, Z. Wang^{1,48}, Z. Y. Wang¹, Ziyi Wang⁵², Zongyuan Wang^{1,52}, D. H. Wei¹², P. Weidenkaff²⁸, F. Weidner⁵⁷, S. P. Wen¹, D. J. White⁵⁵, U. Wiedner⁴, G. Wilkinson⁵⁸, M. Wolke⁶⁴, L. Wollenberg⁴, J. F. Wu^{1,52}, L. H. Wu¹, L. J. Wu^{1,52}, X. Wu^{9,h}, Z. Wu^{1,48}, L. Xia^{60,48}, H. Xiao^{9,h}, S. Y. Xiao¹, Y. J. Xiao^{1,52}, Z. J. Xiao³⁵, X. H. Xie^{38,k}, Y. G. Xie^{1,48}, Y. H. Xie⁶, T. Y. Xing^{1,52}, X. A. Xiong^{1,52}, G. F. Xu¹, J. J. Xu³⁶, Q. J. Xu¹⁴, W. Xu^{1,52}, X. P. Xu⁴⁶, L. Yan^{9,h}, L. Yan^{63A,63C}, W. B. Yan^{60,48}, W. C. Yan⁶⁸, Xu Yan⁴⁶, H. J. Yang^{42,g}, H. X. Yang¹, L. Yang⁶⁵, R. X. Yang^{60,48}, S. L. Yang^{1,52}, Y. H. Yang³⁶, Y. X. Yang¹², Yifan Yang^{1,52}, Zhi Yang²⁵, M. Ye^{1,48}, M. H. Ye⁷, J. H. Yin¹, Z. Y. You⁴⁹,

B. X. Yu^{1,48,52}, C. X. Yu³⁷, G. Yu^{1,52}, J. S. Yu^{20,l}, T. Yu⁶¹, C. Z. Yuan^{1,52}, W. Yuan^{63A,63C}, X. Q. Yuan^{38,k}, Y. Yuan¹, Z. Y. Yuan⁴⁹, C. X. Yue³³, A. Yuncu^{51B,a}, A. A. Zafar⁶², Y. Zeng^{20,l}, B. X. Zhang¹, Guangyi Zhang¹⁶, H. H. Zhang⁴⁹, H. Y. Zhang^{1,48}, J. L. Zhang⁶⁶, J. Q. Zhang⁴, J. W. Zhang^{1,48,52}, J. Y. Zhang¹, J. Z. Zhang^{1,52}, Jianyu Zhang^{1,52}, Jiawei Zhang^{1,52}, L. Zhang¹, Lei Zhang³⁶, S. Zhang⁴⁹, S. F. Zhang³⁶, T. J. Zhang^{42,g}, X. Y. Zhang⁴¹, Y. Zhang⁵⁸, Y. H. Zhang^{1,48}, Y. T. Zhang^{60,48}, Yan Zhang^{60,48}, Yao Zhang¹, Yi Zhang^{9,h}, Z. H. Zhang⁶, Z. Y. Zhang⁶⁵, G. Zhao¹, J. Zhao³³, J. Y. Zhao^{1,52}, J. Z. Zhao^{1,48}, Lei Zhao^{60,48}, Ling Zhao¹, M. G. Zhao³⁷, Q. Zhao¹, S. J. Zhao⁶⁸, Y. B. Zhao^{1,48}, Y. X. Zhao Zhao²⁵, Z. G. Zhao^{60,48}, A. Zhemchugov^{29,b}, B. Zheng⁶¹, J. P. Zheng^{1,48}, Y. Zheng^{38,k}, Y. H. Zheng⁵², B. Zhong³⁵, C. Zhong⁶¹, L. P. Zhou^{1,52}, Q. Zhou^{1,52}, X. Zhou⁶⁵, X. K. Zhou⁵², X. R. Zhou^{60,48}, A. N. Zhu^{1,52}, J. Zhu³⁷, K. Zhu¹, K. J. Zhu^{1,48,52}, S. H. Zhu⁵⁹, W. J. Zhu³⁷, X. L. Zhu⁵⁰, Y. C. Zhu^{60,48}, Z. A. Zhu^{1,52}, B. S. Zou¹, J. H. Zou¹

(BESIII Collaboration)

¹ Institute of High Energy Physics, Beijing 100049, People's Republic of China

² Beihang University, Beijing 100191, People's Republic of China

³ Beijing Institute of Petrochemical Technology, Beijing 102617, People's Republic of China

⁴ Bochum Ruhr-University, D-44780 Bochum, Germany

⁵ Carnegie Mellon University, Pittsburgh, Pennsylvania 15213, USA

⁶ Central China Normal University, Wuhan 430079, People's Republic of China

⁷ China Center of Advanced Science and Technology, Beijing 100190, People's Republic of China

⁸ COMSATS University Islamabad, Lahore Campus, Defence Road, Off Raiwind Road, 54000 Lahore, Pakistan

⁹ Fudan University, Shanghai 200443, People's Republic of China

¹⁰ G.I. Budker Institute of Nuclear Physics SB RAS (BINP), Novosibirsk 630090, Russia

¹¹ GSI Helmholtzcentre for Heavy Ion Research GmbH, D-64291 Darmstadt, Germany

¹² Guangxi Normal University, Guilin 541004, People's Republic of China

¹³ Guangxi University, Nanning 530004, People's Republic of China

¹⁴ Hangzhou Normal University, Hangzhou 310036, People's Republic of China

¹⁵ Helmholtz Institute Mainz, Johann-Joachim-Becher-Weg 45, D-55099 Mainz, Germany

¹⁶ Henan Normal University, Xinxiang 453007, People's Republic of China

¹⁷ Henan University of Science and Technology, Luoyang 471003, People's Republic of China

¹⁸ Huangshan College, Huangshan 245000, People's Republic of China

¹⁹ Hunan Normal University, Changsha 410081, People's Republic of China

²⁰ Hunan University, Changsha 410082, People's Republic of China

²¹ Indian Institute of Technology Madras, Chennai 600036, India

²² Indiana University, Bloomington, Indiana 47405, USA

²³ (A)INFN Laboratori Nazionali di Frascati, I-00044, Frascati, Italy; (B)INFN and University of Perugia, I-06100, Perugia, Italy

²⁴ (A)INFN Sezione di Ferrara, I-44122, Ferrara, Italy; (B)University of Ferrara, I-44122, Ferrara, Italy

²⁵ Institute of Modern Physics, Lanzhou 730000, People's Republic of China

²⁶ Institute of Physics and Technology, Peace Ave. 54B, Ulaanbaatar 13330, Mongolia

²⁷ Jilin University, Changchun 130012, People's Republic of China

²⁸ Johannes Gutenberg University of Mainz, Johann-Joachim-Becher-Weg 45, D-55099 Mainz, Germany

²⁹ Joint Institute for Nuclear Research, 141980 Dubna, Moscow region, Russia

³⁰ Justus-Liebig-Universitaet Giessen, II. Physikalisches Institut, Heinrich-Buff-Ring 16, D-35392 Giessen, Germany

³¹ KVI-CART, University of Groningen, NL-9747 AA Groningen, The Netherlands

³² Lanzhou University, Lanzhou 730000, People's Republic of China

³³ Liaoning Normal University, Dalian 116029, People's Republic of China

³⁴ Liaoning University, Shenyang 110036, People's Republic of China

³⁵ Nanjing Normal University, Nanjing 210023, People's Republic of China

³⁶ Nanjing University, Nanjing 210093, People's Republic of China

³⁷ Nankai University, Tianjin 300071, People's Republic of China

³⁸ Peking University, Beijing 100871, People's Republic of China

³⁹ Qufu Normal University, Qufu 273165, People's Republic of China

⁴⁰ Shandong Normal University, Jinan 250014, People's Republic of China

- ⁴¹ Shandong University, Jinan 250100, People's Republic of China
⁴² Shanghai Jiao Tong University, Shanghai 200240, People's Republic of China
⁴³ Shanxi Normal University, Linfen 041004, People's Republic of China
⁴⁴ Shanxi University, Taiyuan 030006, People's Republic of China
⁴⁵ Sichuan University, Chengdu 610064, People's Republic of China
⁴⁶ Soochow University, Suzhou 215006, People's Republic of China
⁴⁷ Southeast University, Nanjing 211100, People's Republic of China
⁴⁸ State Key Laboratory of Particle Detection and Electronics, Beijing 100049, Hefei 230026, People's Republic of China
⁴⁹ Sun Yat-Sen University, Guangzhou 510275, People's Republic of China
⁵⁰ Tsinghua University, Beijing 100084, People's Republic of China
⁵¹ (A)Ankara University, 06100 Tandoğan, Ankara, Turkey; (B)Istanbul Bilgi University, 34060 Eyüp, İstanbul, Turkey;
(C)Uludag University, 16059 Bursa, Turkey; (D)Near East University, Nicosia, North Cyprus, Mersin 10, Turkey
⁵² University of Chinese Academy of Sciences, Beijing 100049, People's Republic of China
⁵³ University of Hawaii, Honolulu, Hawaii 96822, USA
⁵⁴ University of Jinan, Jinan 250022, People's Republic of China
⁵⁵ University of Manchester, Oxford Road, Manchester, M13 9PL, United Kingdom
⁵⁶ University of Minnesota, Minneapolis, Minnesota 55455, USA
⁵⁷ University of Muenster, Wilhelm-Klemm-Str. 9, 48149 Muenster, Germany
⁵⁸ University of Oxford, Keble Rd, Oxford, UK OX13RH
⁵⁹ University of Science and Technology Liaoning, Anshan 114051, People's Republic of China
⁶⁰ University of Science and Technology of China, Hefei 230026, People's Republic of China
⁶¹ University of South China, Hengyang 421001, People's Republic of China
⁶² University of the Punjab, Lahore-54590, Pakistan
⁶³ (A)University of Turin, I-10125, Turin, Italy; (B)University of Eastern Piedmont, I-15121, Alessandria, Italy; (C)INFN,
I-10125, Turin, Italy
⁶⁴ Uppsala University, Box 516, SE-75120 Uppsala, Sweden
⁶⁵ Wuhan University, Wuhan 430072, People's Republic of China
⁶⁶ Xinyang Normal University, Xinyang 464000, People's Republic of China
⁶⁷ Zhejiang University, Hangzhou 310027, People's Republic of China
⁶⁸ Zhengzhou University, Zhengzhou 450001, People's Republic of China
^a Also at Bogazici University, 34342 Istanbul, Turkey
^b Also at the Moscow Institute of Physics and Technology, Moscow 141700, Russia
^c Also at the Novosibirsk State University, Novosibirsk, 630090, Russia
^d Also at the NRC "Kurchatov Institute", PNPI, 188300, Gatchina, Russia
^e Also at Istanbul Arel University, 34295 Istanbul, Turkey
^f Also at Goethe University Frankfurt, 60323 Frankfurt am Main, Germany
^g Also at Key Laboratory for Particle Physics, Astrophysics and Cosmology, Ministry of Education; Shanghai Key Laboratory
for Particle Physics and Cosmology; Institute of Nuclear and Particle Physics, Shanghai 200240, People's Republic of China
^h Also at Key Laboratory of Nuclear Physics and Ion-beam Application (MOE) and Institute of Modern Physics, Fudan
University, Shanghai 200443, People's Republic of China
ⁱ Also at Harvard University, Department of Physics, Cambridge, MA, 02138, USA
^j Currently at: Institute of Physics and Technology, Peace Ave.54B, Ulaanbaatar 13330, Mongolia
^k Also at State Key Laboratory of Nuclear Physics and Technology, Peking University, Beijing 100871, People's Republic of
China
^l School of Physics and Electronics, Hunan University, Changsha 410082, China

(Dated: February 12, 2021)

MEASUREMENT OF THE BRANCHING FRACTION OF $\psi(3686) \rightarrow \Omega^- \bar{\Omega}^+$

After applying the event selection described in the main body of the paper, the $M_{K-\Lambda}$ distribution for events within the $M_{K-\Lambda}^{\text{recoil}}$ mass window (Fig. 1(b) in main manuscript) and the $M_{K+\bar{\Lambda}}$ distribution for events within $M_{K+\bar{\Lambda}}^{\text{recoil}}$ mass window (Fig. 1(c) in main manuscript) are fitted simultaneously using the unbinned maximum-likelihood method to determine the branching fraction of $\psi(3686) \rightarrow \Omega^- \bar{\Omega}^+$ directly. To remove statistical correlations, events containing both a reconstructed Ω^- and an $\bar{\Omega}^+$ are removed from the $M_{K-\Lambda}$ distribution.

The number of signal events in the k th mode (N_k , $k = 1$ for Ω^- and $k = 2$ for $\bar{\Omega}^+$) is

$$N_k = N_{\psi(3686)} \times \mathcal{B}(\psi(3686) \rightarrow \Omega^- \bar{\Omega}^+) \times \mathcal{B}(\Omega \rightarrow K\Lambda) \times \mathcal{B}(\Lambda \rightarrow p\pi^-) \times \varepsilon_k, \quad (1)$$

where $\mathcal{B}(\Omega^- \rightarrow K^- \Lambda)$ and $\mathcal{B}(\Lambda \rightarrow p\pi^-)$ are the branching fractions of Ω^- decays to $K^- \Lambda$ and that of $\Lambda \rightarrow p\pi^-$, respectively, and ε_k is the efficiency determined from the signal MC sample generated with the MDIY generator [1] using the parameters listed in Table I in main manuscript. These efficiencies, after being corrected by the two dimensional tracking and PID efficiency scale factors, are found to be $\varepsilon_1 = 17.1\%$ and $\varepsilon_2 = 18.9\%$.

In the fit for the signal yields, the signal PDF is parametrized by a double Gaussian function with a common mean (M) and two distinct resolutions (σ_1 and σ_2). The background is described by a first-order Chebyshev polynomial. The parameters in the signal PDF (M , σ_1 and σ_2) are free in the fit, but constrained to be the same for the Ω^- and $\bar{\Omega}^+$ signals. The fit (Fig. 1(b) and (c) in main manuscript) returns $N_1 = 1966 \pm 54$ and $N_2 = 2069 \pm 54$. The average value of $\mathcal{B}(\psi(3686) \rightarrow \Omega^- \bar{\Omega}^+)$ for these two single-tag samples is determined to be $(5.85 \pm 0.12) \times 10^{-5}$, where the uncertainty is statistical only.

The following sources of systematic uncertainties are considered for the branching fraction measurement.

The method described above for determining the systematic uncertainties for the angular distribution analysis is used for the tracking and PID efficiency correction, and the uncertainty is 1.4%. The uncertainties due to the mass windows requirements of $M_{p\pi}$ and $M_{K\Lambda}^{\text{recoil}}$ are estimated by comparing the efficiency difference of the requirements between data and MC simulations, which are 0.7% and 0.7% for $\Lambda(\bar{\Lambda})$ and $\Omega^-(\bar{\Omega}^+)$, respectively. The uncertainties in $\mathcal{B}(\Omega^- \rightarrow K^- \Lambda)$ and $\mathcal{B}(\Lambda \rightarrow p\pi^-)$ are taken from the PDG [2] and the sum in quadrature is 1.3%. The uncertainty of the number of $\psi(3686)$ events is 0.6% [3]. The uncertainties from the input α_{Ω^-} and α_Λ are estimated by changing these two parameters by 1σ standard deviation, and are found to be 1.0% and 1.2%, respectively.

The uncertainty arising from the helicity parameters, h_i , ϕ_i , and ϕ_{Ω^-} , is estimated with 100 groups of random values of these seven parameters are sampled from a multi-normal distribution with the means and covariance matrix as measured in data. A MC sample generated with a phase space model is weighted with these new parameters and subsequently new detection efficiencies and new branching fractions are obtained by repeating the fit to the $K^- \Lambda$ invariant-mass distributions. The standard deviation of the branching fraction distribution of these 100 MC samples, 1.6%, is taken as the uncertainty.

The uncertainty from the signal shape is obtained by replacing the double Gaussian with the MC simulated shape convolved with a Gaussian function to account for the resolution difference between data and MC simulation, and 2.0% is taken as the systematic uncertainty. The uncertainty due to the background shape is estimated by changing the first-order to a second-order Chebyshev polynomial, which leads to a uncertainty of 1.8%.

The contributions from these sources are added in quadrature, and a total relative systematic uncertainty in $\mathcal{B}(\psi(3686) \rightarrow \Omega^- \bar{\Omega}^+)$ of 4.3% is obtained.

The branching fraction for $\psi(3686) \rightarrow \Omega^- \bar{\Omega}^+$ is measured to be $(5.85 \pm 0.12 \pm 0.25) \times 10^{-5}$, where the first uncertainty is statistical, and the second is systematic. This result agrees with previous measurements [4, 5] with improved precision.

- [1] R. G. Ping, Chin. Phys. C **32**, 599 (2008).
- [2] M. Tanabashi *et al.* (Particle Data Group), Phys. Rev. D **98**, 030001 (2018).
- [3] M. Ablikim *et al.* (BESIII Collaboration), Chin. Phys. C **42**, 023001 (2018).
- [4] S. Dobbs, A. Tomaradze, T. Xiao, K. K. Seth and G. Bonvicini, Phys. Lett. B **739**, 90 (2014).
- [5] S. Dobbs, K. K. Seth, A. Tomaradze, T. Xiao and G. Bonvicini, Phys. Rev. D **96**, 092004 (2017).

STATISTICAL AND SYSTEMATIC COVARIANCE MATRICES FOR THE TWO SOLUTIONS

TABLE I. The statistical covariance matrix for solution I.

parameter	h_1	ϕ_1	h_3	ϕ_3	h_4	ϕ_4	ϕ_{Ω^-}
h_1	0.012	-0.030	0.004	-0.002	0.0006	-0.045	-0.001
ϕ_1	-0.030	0.171	-0.011	0.010	-0.001	0.107	-0.032
h_3	0.004	-0.010	0.003	-0.002	0.0003	-0.0180	0.001
ϕ_3	-0.002	0.010	-0.002	0.027	0.0003	0.020	-0.002
h_4	0.0006	-0.001	0.0003	0.0003	0.0007	-0.0005	0.0009
ϕ_4	-0.045	0.107	-0.018	0.020	-0.0005	0.684	0.123
$\phi_{\Omega^-}/\phi_{\bar{\Omega}^+}$	-0.001	-0.032	0.001	-0.002	0.0009	0.123	0.200

TABLE II. The statistical covariance matrix for solution II.

parameter	h_1	ϕ_1	h_3	ϕ_3	h_4	ϕ_4	ϕ_{Ω^-}
h_1	0.011	0.023	0.004	-0.003	0.0006	0.023	-0.009
ϕ_1	0.023	0.139	0.008	-0.002	0.001	0.015	-0.006
h_3	0.004	0.008	0.003	-0.003	0.0004	0.008	-0.002
ϕ_3	-0.003	-0.002	-0.003	0.027	0.0002	0.011	0.015
h_4	0.0006	0.001	0.0004	0.0002	0.0007	0.002	0.0005
ϕ_4	0.023	0.015	0.008	0.011	0.002	0.467	-0.078
$\phi_{\Omega^-}/\phi_{\bar{\Omega}^+}$	-0.009	-0.006	-0.002	0.015	0.0005	-0.078	0.198

TABLE III. The combined statistical and systematic covariance matrix for solution I.

parameter	h_1	ϕ_1	h_3	ϕ_3	h_4	ϕ_4	ϕ_{Ω^-}
h_1	0.017	-0.038	0.004	-0.002	0.0009	-0.058	-0.002
ϕ_1	-0.038	0.194	-0.012	0.012	-0.002	0.120	-0.038
h_3	0.004	-0.011	0.003	-0.002	0.0004	-0.019	0.001
ϕ_3	-0.002	0.017	-0.002	0.032	0.0004	0.024	-0.003
h_4	0.0009	-0.002	0.0004	0.0009	-0.0006	0.001	
ϕ_4	-0.058	0.120	-0.019	0.024	-0.0006	0.810	0.150
$\phi_{\Omega^-}/\phi_{\bar{\Omega}^+}$	-0.002	-0.038	0.001	-0.003	0.001	0.150	0.250

TABLE IV. The combined statistical and systematic covariance matrix for solution II.

parameter	h_1	ϕ_1	h_3	ϕ_3	h_4	ϕ_4	ϕ_{Ω^-}
h_1	0.012	0.026	0.004	-0.003	0.0007	0.025	-0.011
ϕ_1	0.026	0.160	0.008	-0.002	0.001	0.016	-0.007
h_3	0.004	0.008	0.003	-0.003	0.0004	0.009	-0.002
ϕ_3	-0.003	-0.002	-0.003	0.029	0.0002	0.011	0.017
h_4	0.0008	0.001	0.0004	0.0002	0.0009	0.002	0.0006
ϕ_4	0.025	0.016	0.007	0.011	0.002	0.490	-0.086
$\phi_{\Omega^-}/\phi_{\bar{\Omega}^+}$	-0.011	-0.007	-0.002	0.017	0.0006	-0.086	0.230